IRAQI Academic Scientific Journals

Samarra Journal of Pure and Applied Science

SJPAS

www.sjpas.com

p ISSN: 2663-7405
e ISSN: 2789-6838

Effect of Polarization on Nonlinear Optical Properties of ZnO Thin Film

Tharaa Jirjees Polus [1]*, Thoalfiqar Ali Zaker [2,3], Ammar Tahssen Zakar [1] and Yasir Hussein Mohammed[1]

1- Department of Physics, College of Education for Pure Sciences, Mosul University, Mosul, 41002, Iraq
2- Department of Physics, College of Education, University of Al-Hamdaniya, Nineveh, 41006, Iraq
3- Laser & Spectroscopy Department, Laser & Photonics Research Center, University of Al-Hamdaniya, Nineveh, 41006, Iraq

https://doi.org/10.54153/sjpas.2021.v3i4.315

Article Information

Received: 26/08/2021
Accepted: 13/10/2021

Keywords:

ZnO thin films, Z-scan technique, Polarization, Nonlinear properties.

Corresponding Author

E-mail: tharaasony23@gmail.com
Mobile:

Abstract

The dependency of the 3rd order nonlinear optical properties of the Zinc Oxide (ZnO) thin films on laser light polarization were investigated with the widely known Z-scan technique. The measurements were taken at linearly, elliptically, and circularly polarized light at both P-polarization and S-polarization states. Pulse-wave red diode laser diode at repetition rate of 1 KHz, wavelength of 650 nm and maximum power of 3mW was used. The laser beam passes through a thin film sample with thickness of (425nm). The sample was deposited on the glass substrates using atmospheric pressure chemical vapor deposition (APCVD) technique. The measurements of NLR and NLA indicates that the linearly polarized light has the largest values. The circularly polarized light has the smallest values for both P- and S-polarization. Also, the ZnO thin films exhibit a better nonlinearity at S-polarization in comparison to P-polarization. The high nonlinearity can lead for using the material in many applications.

Introduction:

Nonlinear phenomena gained wide intention and used in many research in a short amount of time [1]. These phenomena contribution in many applications such as in optoelectronic and photonic devices [2]. It has been used to generate THz radiation and the studies were done by taken the wavelength range from infrared to extreme UV [3]. Nonlinear optics studied an intense laser light interaction with matter [4], which leads to a change in the optical behaviour of a medium [5]. The nonlinear optical (NLO) materials exhibit a nonlinear optical effect [6] when placing in front of a laser beam path.

Zinc Oxide (ZnO) thin films is an inorganic [7], II-VI compound semiconductor material with a wide band gap of 3.37 eV at room temperature [8]. Making the material a great candidate in NLO-based devices [9]. It has a strong binding energy of 60 meV [10]. ZnO is transparent in the visible region [11] which is used in applications such as, transparent conductive films and window materials in solar cell applications [12].

There are various techniques for investigation the nonlinear properties including, degenerate four wave mixing (DFWM) [13], interferometry measurements [14], and the Z-scan method. A well-known Z-scan technique was reported by Mansoor Sheik-Bahae et al. [15]. It stood out among other techniques due to its high sensitivity, accuracy, simplicity, and ease of separating both the nonlinear refractive (NLR) index and nonlinear absorption (NLA) coefficient. Various modification has been employed to this method such as, eclipsing Z-scan (EZ-scan) [16], top-hat-beam Z-scans [17], off-axis Z-scan [18], and time-resolved pump-probe Z-scan [19]. In all of these modifications, a linear polarized light was used [20].

The polarization effects studies progressively became essential in laser physics, spectroscopy, optoelectronics, and optical telecommunications [21]. Various NLO materials were used in the past years to detect the polarization effects [22]. The studies on polarization effects starts with P. R. Monson in 1970s [23]. R. DeSalvo et al., were among the first to study the polarization effects using Z-scan technique. They studied the polarization dependence of NLR index in crystals with linearly polarized light [24]. The first studies were done only by a linearly polarized light until 2007, when Liang et al. used different polarized beams to study the polarization dependence effects of refractive index change (RIC) for PMMA films [25]. The dependency of NLO properties of materials on the incident laser beam polarization is made by placing λ/4 plate into the Z-scan setup before the sample [26]. The polarization effect was chosen in this study because of the random and lack of researches in this field at very low laser power that is used. Besides using the mentioned material as well.

Simplest polarized single light beam Z-scan technique have been used, also referred as one beam Z-scan technique (OBZT) [27]. Both NLR and NLA indices were measured at the two different polarizations states, which are the P- and S-polarization. With using a pulse laser at wavelength of 650 nm, maximum power of 3 mW and frequency of 1 KHz. Also, measurement for the third-order nonlinear optical susceptibility were provide.

Experiment Setup:

The NLO properties of the ZnO thin films (TFs) were measured by using the widely-known Z-scan method based on open aperture and closed aperture. Zinc oxide (ZnO) TFs were deposited on glass (2.5×2.5 cm^2) substrates by atmospheric pressure chemical vapor deposition (APCVD) method [28]. For the growth of ZnO TFs, high-purity Zn acetate dehydrate [$Zn(CH_3COO)_2\cdot2H_2O$] was used as the source of Zn metal. Glass substrates were degreased in successive rinses with acetone, methanol and distilled water for 10 min in each solution. Finally, cleaned substrates were dried using hot air. ZnO TFs were deposited for 20 min at temperature of 500 °C. Balance method was exploited to measure the thickness of TFs, which estimated to be ~425 nm. Tint of light rainbow coating was found on the surface of the glass substrates at the end of the growth process. This represents a visual contact indication of the success of the growth process.

The experimental setup scheme and picture for the Z-scan technique is shown in figure (1) and (2). The sample was moved along the axis using an ARDUINO controlled rotational stage. Where an ARDUINO’s electronic board has been linked to a stepper motor, in which the rotation of the motor has been taken for every 1 mm along the axis. It was used to easily collect data with high accuracy. The sample is moved through the incident laser path as it get closer to the focus. A continues-wave red laser diode with wavelength of 650 nm and maximum power of 3 mW was used as a light source. A function generator used to convert the CW laser to a pulse laser at a fixed frequency of 1 KHz.

A lens with focal length of ~30 mm placed in front of the sample to focus the polarized laser beam on the sample. The beam falls on an aperture with diameter of 0.5 mm. A measurement has been taken by using edge knife technique for the polarized laser beam waist radius ($w_\circ$), and estimated to be ~27 µm. From equation (1), the Rayleigh length can be determined and found to be (3.52 mm).

$$Z_R = \frac{\pi w_\circ^2}{\lambda} \qquad (1)$$

Where Z_R is the Rayleigh length, λ is the laser wavelength.

The polarized laser beam detected using Silicon photo-detector (DET10A). The temperature changes can affect optical cavity dimensions and the behavior of the gain and may change the material's nonlinearity. Many laser diode parameters, such as wavelength, threshold current and efficiency are dependent on the temperature. Therefore, stable temperature control is required, the accuracy of the used controller is of ±0.05 °C.

The investigation of the laser polarization was done at linearly, elliptically, and circularly polarized light. The polarizer used to obtain the nonlinearity indices at the linearly polarized light. The quarter wave-plate (λ/4) used to get the nonlinearity indices at the elliptically and circularly polarized light, as it used to convert the linearly polarized light to circularly polarized light and vice versa. By changing the angle on the λ/4 wave-plate one can convert circularly polarized light to elliptically polarized light.

The SR830 DSP Lock-in-Amplifier used in the setup. Accurate measurements may be made even when a small signal is obscured by noise source many thousands of times large. The Lock-in-Amplifier uses a technique known as phase-sensitive detection (PSD) to single out the component of the signal at a specific reference frequency and phase. Noise signals at frequencies other than reference frequency are rejected and do not affect the measurement.

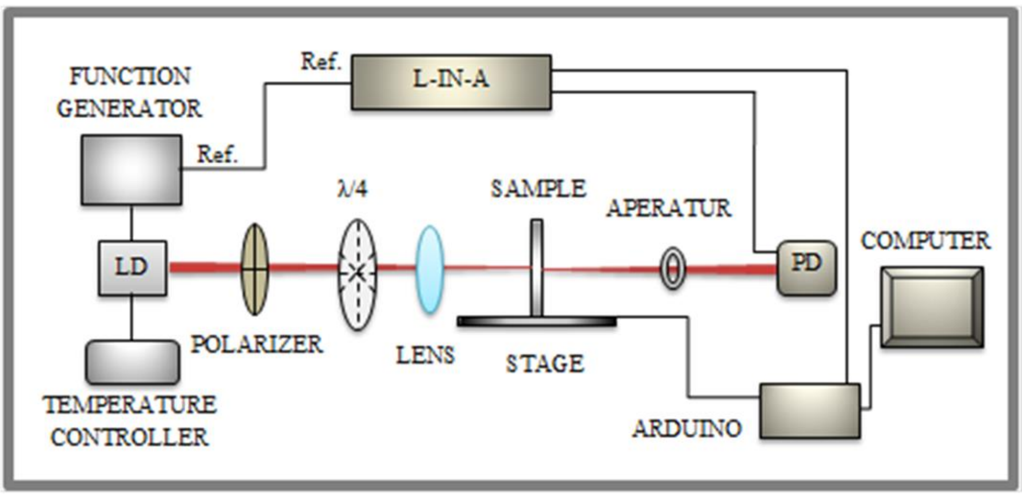

Fig. 1 *The experimental setup for the polarization Z-scan method. The rotational stage is used to move the sample on the axis, LD is a laser diode, λ/4 is a quarter wave-plate, L-IN-A is a Lock-in-Amplifier, and PD is a photo-detector.*

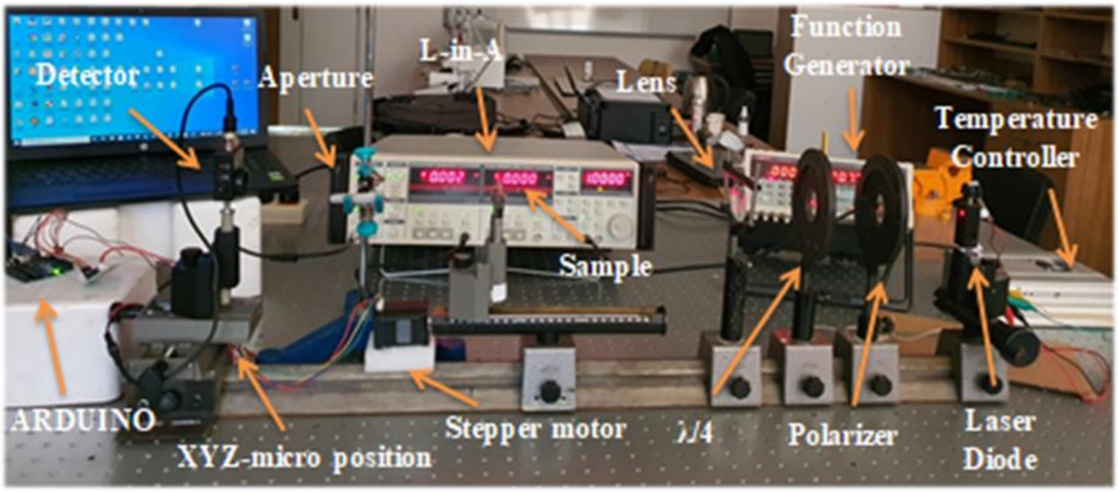

Fig. 2 *Picture for the polarization Z-scan method*

Results and Discussion:

From the Z-scan experimental setup shown in figure (1), the measurements for the two-photon absorption coefficient (2PA or TPA) and refractive index also called as the Kerr effect [29] were done. This method provides two detection method which are the open aperture and closed aperture configurations. In which it detects the 2PA and Kerr effect respectively. At open aperture Z-scan technique the polarized light will transmitted through the sample and directly reaches the detector. In which the NLA coefficient can be measured. In order to measure the NLA coefficient, the determination of the linear absorption coefficient is needed. By using equation (2) the linear absorption coefficient has been obtained [30]. The material absorbance was taken at different wavelengths with the use of an EMC-11D-V spectrophotometer, as it is shown in figure (3).

$$\alpha_\circ = 2.303\frac{A}{L} \qquad (2)$$

Where $\alpha_\circ$ is linear absorption coefficient; A is the material's absorbance and L is the sample's thickness.

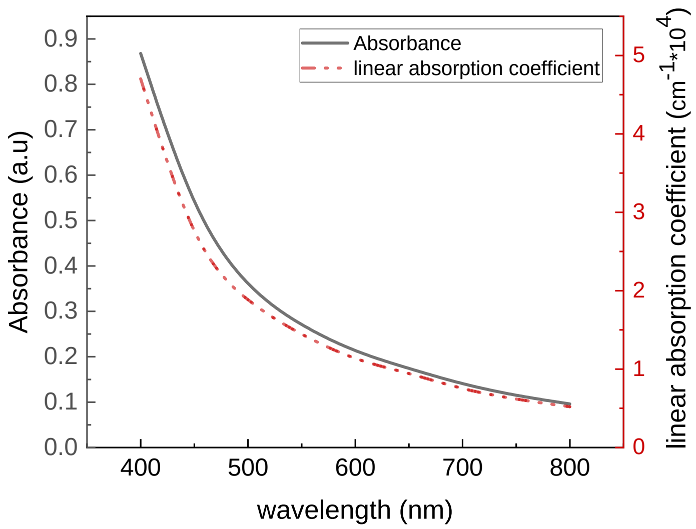

Fig. 3 *Linear absorption coefficient and the absorption spectra of ZnO thin films.*

Figure 3, shows the absorption measurements that were taken from (400-800 nm). Both of the linear absorption coefficient and the material's absorbance measurements that exhibit an exponential decreasing in their values along with increasing the wavelength. This decreasing is due to scattering of the incident light by the material's particles[31].

A measurement of the polarized laser beam transmission was taken at different sample positions through the on-axis, different angles of polarization, and at both P- and S-polarization states. The laser intensity and frequency were taken at fixed values of 2.5 mW and 1KHz respectively.

Firstly, the open aperture data at P-polarization were taken at linearly polarized light at (0°), elliptically polarized light at (30°), and circularly polarized light at (45°), as it is shown in figure (4). In addition, the S-polarization measurements also have been taken at linearly, elliptically, and circularly polarized laser light with angles of 0°, 30°, 45° respectively, as it is shown in figure (5).

The transmission of the polarized beam will reach its minimum value when the sample reaches the focus. The deviation in the laser intensity of the transmitted radiation is due the two-photon-absorption process (TPA). The data illustrated in figure (4) and (5) were fitted using the followed equation [32], in which the nonlinear absorption coefficient β can be obtained.

$$T(z) = [1 + q_{\circ}(z)]/q_{\circ}(z) \qquad (3)$$

Here,

$$q_{\circ} = \frac{\beta I_{\circ}\left[\frac{1-\exp(-\alpha_{\circ}L)}{\alpha_{\circ}}\right]}{1+(\frac{Z}{Z_{\circ}})^2} \qquad (4)$$

Where $I_{\circ}$ is the laser intensity at the focus and can be obtained from the expression $I_{o} = \frac{2P}{\pi w_{o}^{2}}$.

The open aperture configuration for both P- and S-polarization exhibited a valley shape. In which it indicates a positive value of the NLA coefficient (β) related to the TPA process as it was mentioned earlier. The values of β for both polarization cases are the largest at linearly polarized beam followed by elliptically polarized beam as it continues to decrease until it reaches its lowest value at circularly polarized beam, as it is shown in table 1 and 2. By comparing the β values for the P and S-polarization, the β values for S-polarization are much greater than those in P-polarization.

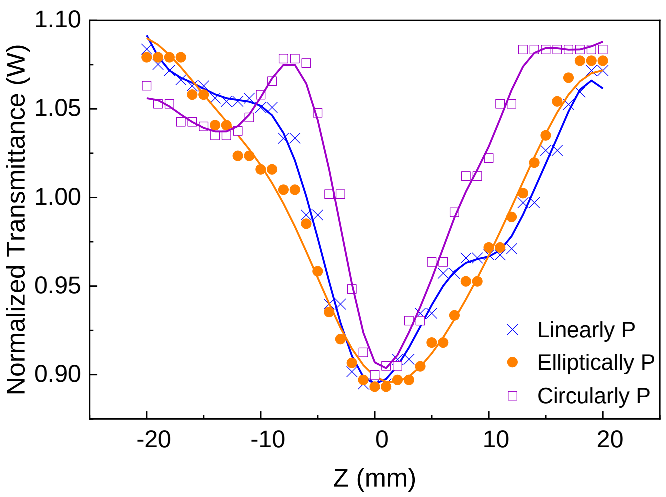

Fig. 4 *Normalized transmittance curves at open-aperture Z-scan for ZnO thin films at different P-polarization.*

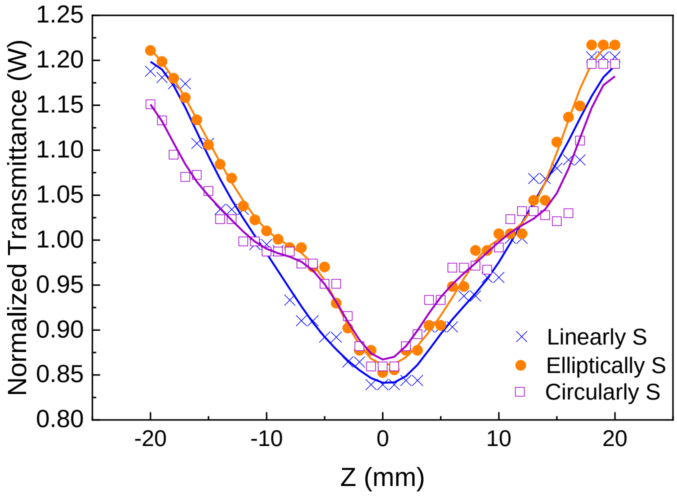

Fig. 5 *Normalized transmittance curves at open-aperture Z-scan for ZnO thin films at different S-polarization.*

An aperture was placed in front of the detector in order to measure the NLR index (n_2). As in the open aperture, we took the data at both P- and S-polarization each at different angles of polarized light which are linearly, elliptically, and circularly polarized laser light with angles of 0°, 30°, 45° respectively, as it is shown in figure (6) and (7). The Kerr indices were obtained by fitting the measurements data to the following equation [32].

$$T(z) = 1 + \frac{4\Delta\phi(I_\circ)_\circ^{(3)}.\frac{z}{z_\circ}}{\left[\left(\frac{z}{z_\circ}\right)^2+9\right].\left[\left(\frac{z}{z_\circ}\right)^2+1\right]} \qquad (5)$$

Here,

$$\Delta\phi(I_\circ)_\circ^{(3)} = K\Delta n\left[\frac{1-\exp(-\alpha_\circ L)}{\alpha_\circ}\right] \qquad (6)$$

Where $\Delta\phi(I_\circ)_\circ^{(3)}$ is the phase shift introduced by the third-order nonlinear optical effects, K is the wave number obtained from $K = 2\pi/\lambda$, and $\Delta n = n_2\, I_\circ$ is the change in the nonlinear refractive index.

The closed aperture data measurements for P-polarization as it is shown in figure (6), exhibit a peak-to-valley shape. Indicating a positive value for the NLR index n_2 ($n_2 > 0$); as it is shown in table 1. The positive values are related to the self-focusing action in which the sample acts as a focusing lens for the incident polarized laser beam. The obtained NLR values from the fitting curves indicates that the NLR for linearly polarized light is the largest than the NLR indices for elliptically and circularly polarized lights. In which they are compatible with Liang's results [25]. The change in NLR's values is related also to the difference of the peak-valley ($\Delta T_{P\text{-}V}$). Furthermore, the measurements for S-polarization state that are illustrated in figure (7) are exhibiting a valley-to-peak shape. Indicating a negative value for the NLR index n_2 ($n_2 < 0$); as it is shown in table 2. The negative values are related to the self-defocusing action. Likewise, the lineally polarized light has the largest values of n_2 followed by the elliptically and then the circularly polarized lights.

In the comparison of the two polarization cases, the difference in values of the RIC is a result to RIC is highly depended on laser beam polarization. That is a consequence to the anisotropy of the 3rd order nonlinear optical susceptibility [22].

As a result of using low laser intensity, the change in polarization values for the same state and for both β and n_2 measurements would be slightly different from each other especially in its valleys or peaks. In some cases, the polarization curves may overlap, but it can be seen in a wide difference in curves at some points. ZnO TFs has a better nonlinearity at S-polarization in comparison to that at P-polarization state. a higher nonlinearity of a material can leads for using it in many applications.

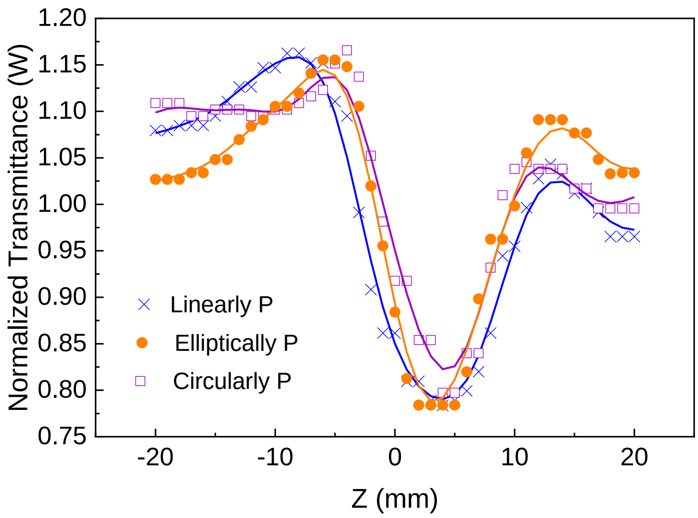

Fig. 6 *Normalized transmittance curves at closed-aperture Z-scan for ZnO thin films at different P-polarization.*

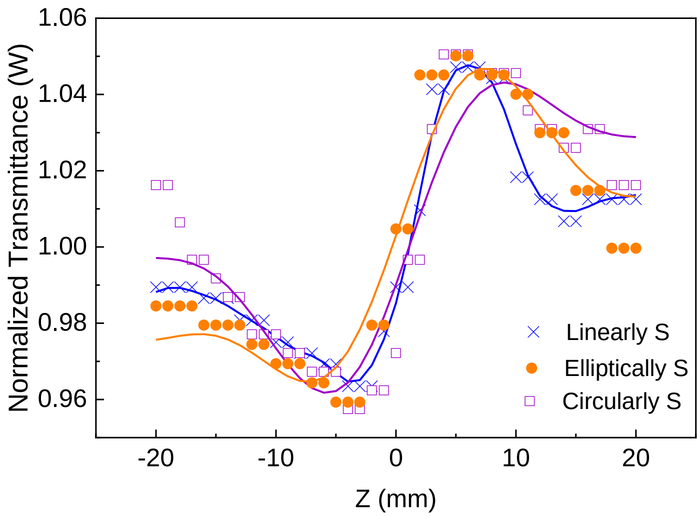

Fig. 7 *Normalized transmittance curves at closed-aperture Z-scan for ZnO thin films at different S-polarization.*

The measurements for the third-order NLO susceptibility ($\chi^{(3)}$) can be obtained as follows [33]:

$$|\chi^{(3)}| = \left[\left(Re(\chi^{(3)})\right)^2 + \left(Im(\chi^{(3)})\right)^2\right]^{\frac{1}{2}} \quad (7)$$

Where $Re(\chi^{(3)})$ is the real part of the third-order NLO susceptibility related to the NLR index, it can be determined from the followed expression [34]:

$$Re(\chi)^{(3)} = \left(\frac{10^{-4} n_o^2 \varepsilon_o c^2}{\pi}\right) n_2 \quad (8)$$

and $Im(\chi^{(3)})$ is the imaginary part of NLO susceptibility that is related to the TPA coefficient, and it can be determined from the followed equation [34]:

$$Im(\chi)^{(3)} = \left(\frac{10^{-2} n_o^2 \varepsilon_o c^2 \lambda}{4\pi^2}\right) \beta \quad (9)$$

Where n_o is the linear refractive index of the material, ε_o is the permittivity of the vacuum, c is the speed of light in vacuum.

Table 1: The extracted values of the nonlinear optical indices and the third-order nonlinear optical susceptibility for the ZnO thin films at P-polarization with different polarized lights.

P-Polarized Light	Nonlinear absorption coefficient β cm/W	Nonlinear refractive index n_2 *10^{-3} cm^2/W	Imaginary part of nonlinear susceptibility Im ($\chi^{(3)}$) *10^{-2} esu	Real part of nonlinear susceptibility Re ($\chi^{(3)}$) esu	Nonlinear susceptibility $\chi^{(3)}$ esu
Linearly	30.00738	-1.1	1.588	-0.112	1.591
Elliptically	29.42788	-1.04	1.557	-0.106	1.56
Circularly	22.80799	-1	1.2	-0.102	1.2

Table 2: The extracted values of the nonlinear optical indices and the third-order nonlinear optical susceptibility for the ZnO thin films at S-polarization with different polarized lights.

S-Polarized Light	Nonlinear absorption coefficient β cm/W	Nonlinear refractive index n_2 *10^{-4} cm^2/W	Imaginary part of nonlinear susceptibility Im ($\chi^{(3)}$) *10^{-2} esu	Real part of nonlinear susceptibility Re ($\chi^{(3)}$) *10^{-2} esu	Nonlinear susceptibility $\chi^{(3)}$ esu
Linearly	58.38104	2.97863	3.09	3.046	4.338
Elliptically	55.98091	2.76483	2.963	2.827	4.095
Circularly	53.77973	2.69112	2.846	2.752	3.958

Conclusions:

Both NLR and NLA were studied as functions of the laser polarization state. The measurement of the third-order NLO susceptibility for the ZnO TFs was provide by using the Z-scan technique. The data were extracted at two states of laser polarization, which are P-polarization and S-polarization. The data were at different polarized laser beams with different angles for each state. The extracted results show a positive sign for NLA coefficient with a largest value at linearly polarized light and a smallest at circularly polarized light. For NLR index, both self-focusing and self-defocusing occurs at P- and S-polarization respectively. With largest values at linearly polarized light and a smallest at circularly polarized light. The obtained results were taken at very low laser intensity which are consistent with the results of another research taken at high laser intensity.

References

1. Suresh, S., Ramanand, A., Jayaraman, D., & Mani, P. (2012). Review on theoretical aspect of nonlinear optics. *Rev. Adv. Mater. Sci*, *30*(2), 175-183.
2. Radhi, F. (2012). Nonlinear responses and optical limiting behavior of 2-Chloro-5-nitroanisole dye under CW laser illumination. *journal of kerbala university*, *8*(2), 181-186.
3. Garmire, E. (2011). Resource letter NO-1: nonlinear optics. *American Journal of Physics*, *79*(3), 245-255. doi: 10.1119/1.3534835
4. Boyd, R. W. (2020). Nonlinear optics. Academic press.
5. De Araújo, C. B., Gomes, A. S., & Boudebs, G. (2016). Techniques for nonlinear optical characterization of materials: a review. Reports on Progress in Physics, 79(3), 036401.
6. Al-Saidi, I. A. D. H., & Abdulkareem, S. A. D. (2015). Nonlinear optical properties and optical power limiting of Leishman dye using z-scan technique. Journal of Materials Science: Materials in Electronics, 26(5), 2713-2718.
7. Khalfa, E. F., Nafaee, Z. H., Abdullah, F. N., Bdair, G. S., Niema, R. M., Salman, H. D., & Hussein, F. H. (2019). Synthesis and Characterizations of Zinc Oxide Nanoparticles-Loaded Chloramphenicol for Antibacterial Applications. Annals of Tropical Medicine and Public Health, 22, 165-176. doi: 10.36295/ASRO.2019.221217
8. Abed, S., Bouchouit, K., Aida, M. S., Taboukhat, S., Sofiani, Z., Kulyk, B., & Figa, V. (2016). Nonlinear optical properties of zinc oxide doped bismuth thin films using Z-scan technique. Optical Materials, 56, 40-44. doi: 10.1016/j.optmat.2015.12.014
9. Irimpan, L., Nampoori, V. P. N., Radhakrishnan, P., Krishnan, B., & Deepthy, A. (2008). Size-dependent enhancement of nonlinear optical properties in nanocolloids of ZnO. Journal of applied physics, 103(3), 033105. doi: 10.1063/1.2838178
10. Hussain, S. (2008). Investigation of structural and optical properties of nanocrystalline ZnO. PhD Thesis, Linköping University.
11. Sun, X. W., & Kwok, H. S. (1999). Optical properties of epitaxially grown zinc oxide films on sapphire by pulsed laser deposition. Journal of applied physics, 86(1), 408-411. doi: 10.1063/1.370744
12. Faraj, M. G., & Ibrahim, K. (2011). Optical and structural properties of thermally evaporated zinc oxide thin films on polyethylene terephthalate substrates. *International Journal of Polymer Science*, *2011*. doi: 10.1155/2011/302843
13. Sutherland, R. L. (1996). Handbook of Nonlinear Optics, Marcel Dekker. New York.
14. Saltiel, S. M., Van Wonterghem, B., & Rentzepis, P. M. (1989). Measurement of χ (3) and phase shift of nonlinear media by means of a phase-conjugate interferometer. Optics letters, 14(3), 183-185. doi: 10.1364/OL.14.000183
15. Sheik-Bahae, M., Said, A. A., Wei, T. H., Wu, Y. Y., Hagan, D. J., Soileau, M. J., & Van Stryland, E. W. (1990, January). Z-scan: a simple and sensitive technique for nonlinear refraction measurements. In Nonlinear Optical Properties Of Materials (Vol. 1148, pp. 41-51). International Society for Optics and Photonics. doi: 10.1117/12.962142
16. Xia, T., Hagan, D. J., Sheik-Bahae, M., & Van Stryland, E. W. (1994). Eclipsing Z-scan measurement of λ/10 4 wave-front distortion. Optics letters, 19(5), 317-319. doi: 10.1364/OL.19.000317

17. Zhao, W., & Palffy-Muhoray, P. (1994). Z-scan measurement of χ (3) using top-hat beams. Applied physics letters, 65(6), 673-675. doi: 10.1063/1.112264
18. Tian, J. G., Zang, W. P., & Zhang, G. (1994). Two modified Z-scan methods for determination of nonlinear-optical index with enhanced sensitivity. Optics communications, 107(5-6), 415-419. doi: 10.1016/0030-4018(94)90358-1
19. Wang, J., Sheik-Bahae, M., Said, A. A., Hagan, D. J., & Van Stryland, E. W. (1994). Time-resolved Z-scan measurements of optical nonlinearities. JOSA B, 11(6), 1009-1017. doi: 10.1364/JOSAB.11.001009
20. Yan, X. Q., Liu, Z. B., Zhang, X. L., Zhou, W. Y., & Tian, J. G. (2009). Polarization dependence of Z-scan measurement: theory and experiment. Optics express, 17(8), 6397-6406. doi: 10.1364/OE.17.006397
21. Svirko, Y. P., & Zheludev, N. I. (1998). Polarization of light in nonlinear optics.
22. Yan, X. Q., Liu, Z. B., Chen, Y. S., & Tian, J. G. (2012). Polarization characteristics of nonlinear refraction and nonlinear scattering in several solvents. JOSA B, 29(10), 2721-2728. doi: 10.1364/JOSAB.29.002721
23. Monson, P. R., & McClain, W. M. (1970). Polarization dependence of the two-photon absorption of tumbling molecules with application to liquid 1-chloronaphthalene and benzene. The Journal of Chemical Physics, 53(1), 29-37. doi: 10.1063/1.1673778
24. DeSalvo, R., Sheik-Bahae, M., Said, A. A., Hagan, D. J., & Van Stryland, E. W. (1993). Z-scan measurements of the anisotropy of nonlinear refraction and absorption in crystals. Optics letters, 18(3), 194-196. doi: 10.1364/OL.18.000194
25. Liang, J., Zhao, H., Zhou, X., & Wang, H. (2007). Polarization-dependent effects of refractive index change associated with photoisomerization investigated with Z-scan technique. Journal of applied physics, 101(1), 013106. doi: 10.1063/1.2402582
26. Bundulis, A., Mihailovs, I., & Rutkis, M. (2020). Origin of the Kerr effect: investigation of solutions by polarization-dependent Z-scan. *JOSA B*, *37*(6), 1806-1811. doi: 10.1364/JOSAB.389520
27. Pintle, J. A. D., Lara, E. R., & Castillo, M. D. I. (2013). Sensitivity optimization of the one beam Z-scan technique and a Z-scan technique immune to nonlinear absorption. Optics express, 21(13), 15350-15363.
28. Mohammed, Y. H. (2019). Fabrication of n-MgZnO/p-Si heterojunction diode: Role of magnesium doping. *Superlattices and Microstructures*, *131*, 104-116. doi: 10.1016/j.spmi.2019.06.001
29. Bundulis, A., Nitiss, E., Busenbergs, J., & Rutkis, M. (2018). Mach–Zehnder interferometer implementation for thermo-optical and Kerr effect study. *Applied Physics B*, *124*(4), 1-7.
30. Borhani Zarandi, M., & Amrollahi Bioki, H. (2017). Effects of Cobalt Doping on Optical Properties of ZnO Thin Films Deposited by Sol–Gel Spin Coating Technique. *Journal of Optoelectronical Nanostructures*, *2*(4), 33-44.
31. Walden, S. L., Fernando, J. F., Shortell, M. P., & Jaatinen, E. A. (2020). Accurate determination of nonlinear refraction in ZnO and Au composite nanostructures. Optical Materials Express, 10(2), 653-661.
32. Sheik-Bahae, M., Said, A. A., Wei, T. H., Hagan, D. J., & Van Stryland, E. W. (1990). Sensitive measurement of optical nonlinearities using a single beam. IEEE journal of quantum electronics, 26(4), 760-769. doi: 10.1109/3.53394

33. Mostaghni, F., & Abed, Y. (2018). Synthesis and investigation of nonlinear optical properties of Para Red: Z-scan technique and quantum mechanical calculations. Mat. Sci. Poland, 36, 445-451.

34. Zidan, M. D., Alsous, M. B., Allaf, A. W., Allahham, A., Al-Zier, A., & Rihawi, H. (2016). Z-scan measurements of the third order optical nonlinearity of C60 doped poly (ethylacetylenecarboxylate) under CW regime. *Optik*, *127*(5), 2566-2569. doi: 10.1016/j.ijleo.2015.11.226

IRAQI Academic Scientific Journals

Samarra Journal of Pure and Applied Science

SJPAS
مجلة سامراء للعلوم الصرفة والتطبيقية

www.sjpas.com

p ISSN: 2663-7405
e ISSN: 2789-6838

تأثير الاستقطاب على الخصائص البصرية اللاخطية لغشاء أوكسيد الزنك الرقيق

ثراء جرجيس بولص سوني[1]*، ذو الفقار علي زكر[2،3]، عمار تحسين زكر[1]، ياسر حسين محمد[1]

1- قسم الفيزياء، كلية التربية للعلوم الصرفة، جامعة الموصل، الموصل، العراق

2- قسم الفيزياء، كلية التربية، جامعة الحمدانية، العراق

3- قسم الليزر والاطياف، مركز بحوث الليزر والفوتونيات، جامعة الحمدانية، العراق

البحث مستل من رسالة ماجستير الباحث الاول

معلومات البحث:

تأريخ الاستلام: 2021/08/26
تأريخ القبـــول: 2021/10/13

الكلمات المفتاحية:

رقائق أوكسيد الزنك، تقنية المسح على المحور، الاستقطاب، الخصائص اللاخطية.

معلومات المؤلف

الايميل:tharaasony23@gmail.com
الموبايل:

الخلاصة:

تم دراسة اعتمادية الخصائص البصرية اللاخطية من الرتبة الثالثة لغشاء أوكسيد الزنك الرقيق على استقطاب ضوء الليزر باستخدام تقنية Z-scan. تم اخذ القياسات عند كل من الضوء المستقطب خطياً، بيضوياً ودائرياً وعند كل من حالات الاستقطاب العمودية والافقية. تم استخدام ليزر دايود نبضي احمر اللون ذات معدل تكرار 1 KHz، طول موجي عند 650 nm ويمتلك قدرة عظمى عند 3mW.عينة رقيقة ذات سمك 425 nm تسمح لشعاع الليزر بالمرور من خلالها. تم تحضير العينة من خلال ترسيبها على طبقة من الزجاج باستخدام تقنية ترسيب البخار الكيميائي عند الضغط الجوي (APCVD). قياسات كل من معاملات الامتصاص والانكسار الغير الخطيين بينت أن الضوء المستقطب خطياً يمتلك أعظم قيمة، والضوء المستقطب دائرياً يمتلك أصغر قيمة لكل من حالات الاستقطاب العمودية والأفقية. بالإضافة الى أن رقائق أوكسيد الزنك تظهر لا خطية جيدة عند حالة الاستقطاب العمودي مقارنة مع قيم اللاخطية في حالة الاستقطاب الافقي، حيث أن اللاخطية العالية تؤدي الى امكانية استخدام مادة أوكسيد الزنك في تطبيقات عديدة.